Brownian Diffusion of Hard Spheres at Finite Concentrations

M. Sami Selim and M. A. Al-Naafa
Dept. of Chemical Engineering and Petroleum Refining, Colorado School of Mines, Golden, CO 80401

M. C. Jones
Chemical Engineering Div., National Institute of Standards and Technology, Boulder, CO 80303

We investigated the effect of concentration on the Brownian diffusion of uncharged rigid spheres. Monosize silica spheres were prepared according to the method of Stöber (1968). The particles were sterically stabilized by chemisorption of stearic alcohol at their surface by the method developed by van Helden (1981). Particle radius was 14.5 nm from electron micrographs of the coated particles. Osmotic pressure measurements of the sterically stabilized particles dispersed in cyclohexane showed that the particles behaved as hard spheres. The measurements agreed well with predictions from the Carnahan-Starling equation over the concentration range $0.0458<\phi<0.37$ where ϕ is the volume fraction of the particles in the suspension. Viscosity measurements of silica dispersions were made over the concentration range $0<\phi<0.25$. The relative viscosity over the range $0<\phi<0.2$ was fitted by $\eta_r = 1 + 2.4\phi + 7.1\phi^2$. The coefficients 2.4 and 7.1 in this equation are in good agreement with the theoretical values of 2.5 and 6.2 obtained by Einstein (1906) and Batchelor (1977), respectively. The Brownian diffusion coefficient of the particles dispersed in cyclohexane was measured over the concentration range $0.0055<\phi<0.248$ using Taylor's hydrodynamic stability method. A laser fiber-optic system was used to measure the transient concentration profile along the capillary as indicated by a fluorescent dye. This technique offers the advantage of being direct and nonintrusive. The experimental diffusivity data were found to be well described by the generalized Stokes-Einstein equation (Batchelor, 1976) over the entire concentration range studied.

Introduction

The erratic motion of colloidal particles suspended in liquids is referred to as Brownian motion. For infinitely dilute suspensions and for sufficiently long times, the motion of the particles may be described by a simple diffusion equation. The diffusion constant for the particles, D_0, is given by the familiar Stokes-Einstein relation (Einstein, 1905):

$$D_0 = \frac{k_B T}{f_0} \tag{1}$$

where k_B is Boltzmann's constant, T is absolute temperature, and f_o is the hydrodynamic drag coefficient of a single particle in infinite fluid. For a spherical particle f_o equals $6\pi\eta_0 a$, where η_0 is the viscosity of the suspending liquid and a is the particle radius. The subscript "o" emphasizes that the particle concentration must approach zero for Eq. 1 to be valid. That is, Eq. 1 applies only to suspensions which are so dilute that each particle is effectively alone in infinite fluid. When many particles are present, there are interactions between these particles. The interactions may be direct such as that arising from charge or indirect such as that arising from the motion of the suspending liquid. The hydrodynamic motion of the many particle system may be quite different from that of a single diffusing particle.

Correspondence concerning this article should be addressed to M. Sami Selim.

In recent years, numerous studies have dealt, both theoretically and experimentally, with the Brownian diffusion of interacting particle systems. On the theoretical side, two approaches were adopted; a statistical-mechanical approach and a simple thermodynamic approach (see Table 1). The former is based on the N-particle Smoluchowski equation which describes the instantaneous N-particle distribution function in the configuration space. The thermodynamic approach, on the other hand, ignores the detailed dynamics of colloidal particles, and follows instead Einstein's thermodynamic argument of sedimentation-diffusion equilibrium. In this connection, the most notable work is due to Batchelor (1976) who extended Einstein's thermodynamic argument to finite concentrations and derived a formal expression for the Brownian diffusion coefficient, valid at all concentrations and arbitrary interaction potentials. The resulting generalized Stokes-Einstein relation is given by

$$D(\phi)=\frac{1}{f(\phi)}\frac{\phi}{1-\phi}\left(\frac{\partial\mu}{\partial\phi}\right)_{T,P} \tag{2}$$

where ϕ is the volume fraction of the particles, $\partial\mu/\partial\phi$ is the derivative of the local chemical potential per particle, and represents the thermodynamic driving force for diffusion, $f(\phi)$ is the hydrodynamic frictional coefficient which depends on particle geometry, concentration, and the statistical properties of the particle configuration. This expression must be evaluated with respect to zero-volume flux frame of reference to permit comparison with experiment. Equation 2 could also be expressed in terms of the osmotic pressure, Π, of the suspension. Thus, using the thermodynamic relation:

$$\frac{\phi}{1-\phi}\left(\frac{\partial\mu}{\partial\phi}\right)_{T,P}=\left(\frac{\partial\Pi}{\partial n}\right)_{T,P} \tag{3}$$

Equation 2 becomes

$$D(\phi)=\frac{1}{f(\phi)}\left(\frac{\partial\Pi}{\partial n}\right)_{T,P} \tag{4}$$

where n is the mean number density of the particles. In Batchelor's notation (Batchelor, 1976), Eq. 4 may be written as

$$D=\frac{K(\phi)}{6\pi\eta_0 a}\left(\frac{\partial\Pi}{\partial n}\right)_{T,P} \tag{5}$$

where $K(\phi)$ is the sedimentation coefficient of the particles in the suspension. Note that Eq. 4 separates the hydrodynamic interactions in $f(\phi)$ from the thermodynamic interactions in $\partial\Pi/\partial n$. The former opposes the diffusive motions of the particles while the latter enhances diffusion. The independent contributions of the hydrodynamic and thermodynamic forces in the diffusion process can be elucidated with the rigorous results available in the dilute limit. For uncharged rigid spheres, Batchelor's (1972) result for $K(\phi)$ is

$$K(\phi)=1-6.55\phi+O(\phi^2) \tag{6}$$

and

Table 1. Theoretical Predictions for the Brownian Diffusion Coefficient of Hard Spheres

Authors	D
Simple Thermodynamic Gradient Theories	
Batchelor (1976)	$D_0(1+1.45\phi)$
Berne and Pecora (1976)	$D_0(1+0.45\phi)$
N-Particle Statistical Mechanical Theories	
Altenberger and Deutch (1973)	$D_0(1+2\phi)$
Aguirre and Murphy (1973)	$D_0(1-2.625\phi)$
Anderson and Reed (1976)	$D_0(1-1.83\phi)$
Harris (1976)	$D_0(1+3\phi)$
Hess and Klein (1976)	$D_0(1+\phi)$
Allison et al. (1979)	$D_0(1-2\phi)$
Felderhof (1978)	$D_0(1+1.56\phi)$
Willis (1979)	$D_0(1+1.45\phi)$
Pusey and Tough (1982)	$D_0(1+1.56\phi)$
Glendinning and Russel (1982)	$D_0(1+1.45\phi)$
Phillies (1987)	$D_0(1-0.9\phi)$

$$\left(\frac{\partial\Pi}{\partial n}\right)_{T,P}=k_BT[1+8\phi+O(\phi^2)] \tag{7}$$

so that Eq. 5 becomes

$$\frac{D}{D_0}=(1-6.55\phi)\,(1+8\phi)$$
$$=1+1.45\phi+O(\phi^2) \tag{8}$$

Thus, in the dilute limit, the thermodynamic contribution outweighs the -6.55ϕ from hydrodynamic retardation and D increases modestly with ϕ for $\phi<<1$. It appears that for dilute suspensions, the enhancement of the diffusivity due to the greater availability of particle sites in regions of lower concentration is a little greater than the reduction due to hydrodynamic hindrance to the movement of the particles.

Theoretical analyses based on either the statistical-mechanical approach or the thermodynamic approach predict for hard spheres (that is, in the absence of long-range interactions) that the concentration dependence of $D(\phi)$ is linear when $\phi<<1$ (see Eq. 8). Table 1, however, shows that quite divergent values for the $O(\phi)$ coefficient were found by different authors. The published theoretical predictions for the $O(\phi)$ coefficient in D/D_0 ranged from -2.6 to $+8$ (see Table 1). Felderhof (1978) and Wills (1979) independently confirmed Eq. 8 and discussed the approximate hydrodynamics and/or incomplete physics responsible for the other values. In spite of this affirmation, Phillies (1987) has more recently reported a value of -0.9 for the $O(\phi)$ coefficient.

Most theoretical treatments of the properties of suspensions are restricted to the low density regime where the hydrodynamic interactions between the particles can be assumed to be pairwise additive, that is, only two-body hydrodynamic interactions need be considered. The two-sphere hydrodynamic interactions, however, do not suffice to describe the properties of suspensions at high concentrations. The many-body hydrodynamic interaction problem was addressed by Beenaker and Mazur (1982, 1983) who found up to $O(\phi^2)$.

$$\frac{D}{D_0}=1+1.56\phi+0.91\phi^2 \tag{9}$$

The term of order ϕ is due to two-body hydrodynamic interactions and was derived earlier by Felderhof (1978). The difference between this value and the value of 1.45 due to Batchelor (1976) is due to Felderhof's use of an expansion of the two-sphere mobility functions in inverse powers of the separation of the two spheres in place of the more accurate numerical solution of the two-sphere flow field used by Batchelor. The term of order ϕ^2 in Eq. 9 accounts for three-body interactions. Beenaker and Mazur (1982) showed that a neglect of three-sphere contributions would give a value of -7.58 instead of $+0.91$ for this term. In a concentrated suspension it is therefore essential to fully take into account the many-body hydrodynamic interactions between an arbitrary number of spheres. For further details on the dynamic properties of colloidal suspensions, the reader is referred to the books by R. Pecora (1985), Safran and Clark (1987), Russel et al. (1989), and Schmitz (1990). Other references which are also pertinent include those due to Altenberger (1979), Vrij (1979), Russel (1981), Pusey et al. (1982), Dickinson (1983), Vrij et al. (1983), Pusey and Tough (1985), and Altenberger et al. (1985, 1986, 1987).

Experimental investigations which would provide a test of Brownian diffusion theories are relatively few and contradictory. The majority of these experimental studies were carried out on microemulsions, polymer latexes and proteins in water at relatively high ionic strength, and silica dispersions in non-polar solvents. A summary of the relevant studies is given in Table 2. As can be seen from this table, quite divergent values for the $O(\phi)$ coefficient were provided by the experiments. For instance, we note that analyses of the same Bovin Serum Albumin data by Keller et al. (1971), Anderson and Reed (1976), and Alpert (1976) produced substantially different values for the $O(\phi)$ coefficient ranging from -1.51 to -5.2, and for methemoglobin the same data were interpreted (Alpert, 1976; Keller et al., 1971) to provide a range of coefficients from -0.6 to -2.11. Moreover, the BSA data measured by Keller et al. (1971) differed by as much as a factor of two or more from the data of Phillies et al. (1976). Fair et al. (1978), however, noted that most of these experiments were confounded by residual effects of long-range interaction potentials; thereby making these suspensions unsuitable to model the diffusion of hard spheres. Moreover, these authors and others pointed out to the difficulty in interpreting dynamic light scattering data for large particles. The data of Newman et al. (1974) and Kops-Werkhoven and Fijnaut (1981) appear to be free from both problems. These studies will be discussed further below.

The objective of the present study is to extend the available data on Brownian diffusion of hard spheres to high concentrations and to examine the data in the light of the generalized Stokes-Einstein equation derived by Batchelor (1976). Sterically stabilized silica particles dispersed in cyclohexane are known to behave as hard spheres. The osmotic compressibility

Table 2. Experimental Results for the Brownian Diffusion Coefficient of Hard Spheres

Authors	Solute	Solvent	Method	$O(\phi)$ Coefficient
Keller et al. (1971)	BSA	0.1 M acetate buffer solution at isoelectric pH of 4.7	Diaphragm cell	-1.51
	methemoglobin	0.1 M phosphate buffer solution at isoelectric pH of 7.3	Diaphragm cell	-0.6
Newman et al. (1974)	DNA	0.15 M NaCl-0.015 M sodium citrate (pH 8)	QELS	1.2 ± 0.4
Alpert (1976)	BSA	0.1 M acetate buffer solution at isoelectric pH of 4.7	Diaphragm cell*	-1.81
Alpert and Banks (1976)	Cyanomethemoglobin	0.1 M phosphate buffer solution at isoelectric pH of 7.0	DLS	-0.745
Phillies et al. (1976)	BSA	0.25 M acetate buffer solution at pH 5.0	QELS	-0.564
Anderson and Reed (1976)	BSA	0.1 M acetate buffer solution at isoelectric pH of 4.7	Diaphragm cell*	-5.2
Jones and Johnson (1978)	Oxyhemoglobin A	0.1 M KCl at isoelectric pH of 6.9	DLS	-0.6
	Oxyhemoglobin S	0.1 M KCl at isoelectric pH of 7.1	DLS	-0.6
Fair et al. (1978)	BSA	0.1 M acetate buffer solution at isoelectric pH of 4.7	QELS	-1.48
Kops-Werkhoven and Fijnaut (1981)	Coated Silica particles	cyclohexane	DLS	1.3 ± 0.2
Present work	Coated Silica particles	cyclohexane	Taylor's hydrodynamic stability method	1.39 ± 0.1

* Data by Keller et al. (1971).
Dynamic light scattering (DLS)
Quasi-elastic light scattering (QELS)

of this system was found by van Helden (1981) and Kops-Werkhoven and Fijnaut (1981) to be well described by the Carnahan-Starling equation for hard spheres in particular at high concentrations up to a volume fraction of 40%. This silica system was therefore selected for the present study. The diffusion measurements were made using Taylor's hydrodynamic stability method. In this method, measurements of the marginally stable hydrodynamic condition in a vertical capillary is used to determine the diffusion coefficient of the species whose concentration gradient gives rise to the density inversion. The method was first proposed by Taylor (1954, Appendix), analyzed mathematically by Wooding (1959), and verified experimentally by Lin (1971) who demonstrated by spectroscopic means that the local density gradient at marginal stability is in fact correctly predicted by the linearized mathematical analysis. The technique was later used by Anderson and coworkers (1978, 1982) to determine the diffusion coefficients for a range of solutes from small molecules to colloidal particles. An account of previous work plus a lucid description of the technique have been recently published (Quinn et al., 1986). In the present article we improved on this method by introducing a laser fiber-optic system capable of direct monitoring of the penetration depth and concentration profile of the diffusing species along the capillary vs. time. This technique offers the advantages of being direct and nonintrusive.

Particle Preparation and Characterization

The preparation of silica particles was performed according to the steps described in our earlier article (Al-Naafa and Selim, 1992). The procedure consists of two steps. First, silica particles were prepared in ethyl alcohol according to the method of Stöber et al. (1968). Spherical particles of uniform size were obtained by the hydrolysis of tetraethyl orthosilicate (TEOS) and subsequent condensation of the formed silicic acid with ammonia as catalyst. TEOS/H_2O/ethanol volume ratios of 1:1.25:29.86 were used to produce spheres of radius $a_{EM} = 14.5$ nm. Second, the particles were sterically stabilized by chemisorption of stearyl alcohol at their surface by the method developed by Iler (1957) and subsequently used by van Helden et al. (1981). The esterification time and temperature used were 5 h and 200°C, respectively. These conditions ensured maximum degree of esterification and zero specific hydroxylated surface area. These were determined by analyzing samples for carbon content and adsorption with methyl red as described by Ballard et al. (1961). After chemisorption the particles were dispersed in cyclohexane and purified by repeated dispersion and centrifugation. We have found that extreme care is required in the preparation of the particles. For instance, TEOS must be extremely pure to assure the best results regarding the uniformity and sphericity of the particles. It is also necessary to maintain a well stirred reaction and to introduce the reactant (TEOS) almost instantaneously, so that the nucleation period is restricted in time and separated from the growth period. Furthermore, it is crucial to avoid the introduction of any nucleation sites into the initial reaction mixture, which probably leads to greater polydispersity in the alcosol. Thus, one needs to take extreme care in cleaning glassware that touches the reactants.

Electron micrographs were taken to determine shape, size, and size distribution of the coated particles. From Figure 1, it can be seen that the particles are uniform and fairly spherical. The size and size distribution of the particles were measured from these pictures and are given in Table 3.

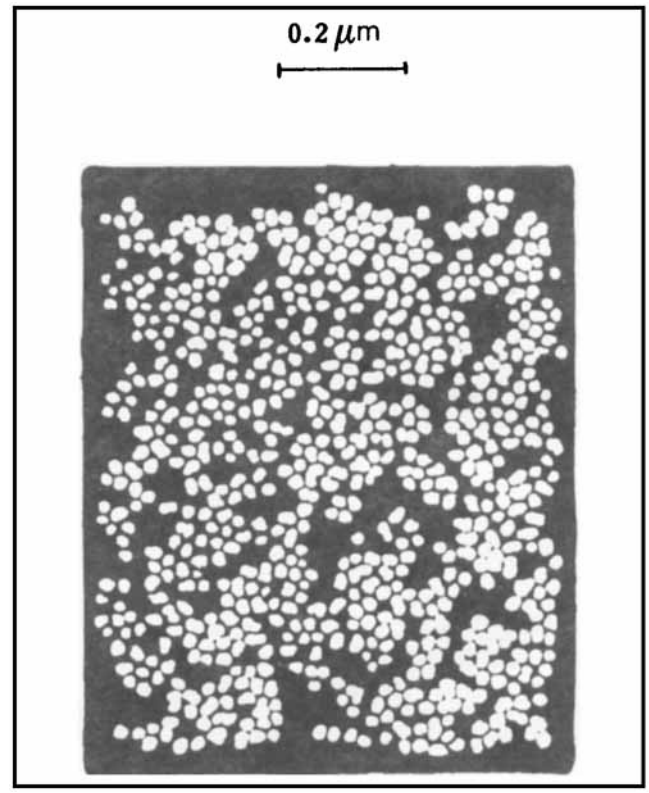

Figure 1. Electron micrograph of coated silica particles with $a_{EM} = 14.5$ nm.

The thermodynamic particle specific volume of the coated particles in cyclohexane were determined from density measurements of silica suspensions with varying particle concentration. The results are shown in Figure 2. From this figure the partial specific volume $\bar{v}_t$ of the particles may be determined using the slope-intercept method (Prigogine and Defay, 1954). As can be seen from this figure the partial specific volume $\bar{v}_t$ is essentially independent of composition in the concentration range $0 < \omega_p < 0.5$ where ω_p is the mass fraction of the particles in the suspension.

The hydrodynamic specific volume $\bar{v}_h$ of the particles was determined from viscosity measurements according to the method suggested by Mewis et al. (1989). The hydrodynamic

Table 3. Properties of Coated Silica Particles

a_{EM} (nm)	$14.50 \pm \sigma$
σ (nm)	1.90
% Standard dev. in size	13.1
a_h (nm)	20.01
$\bar{v}_t$ (cm^3/g)	0.6321
$\bar{v}_h$ (cm^3/g)	0.6892
$D_0 \times 10^8$ (cm^2/s)	12.11 ± 0.03
Esterification temp. (°C)	200
Esterification time (h)	5
% Carbon content (W/W)	12.85
Specific hydroxylated surface area (m^2/g)	0

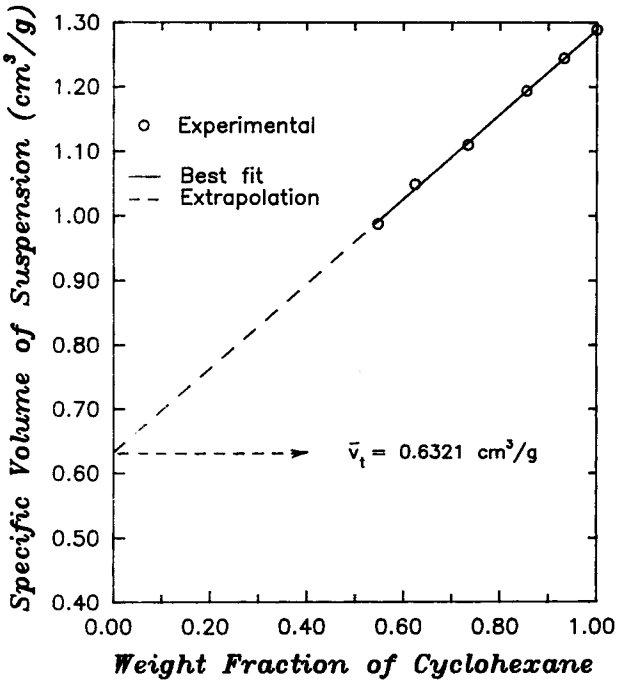

Figure 2. Specific volume of silica suspensions vs. weight fraction of cyclohexane.

specific volume relates the particle volume fraction ϕ to the mass concentration C according to:

$$\phi = \bar{v}_h C \tag{10}$$

Viscosity measurements were performed on silica suspensions

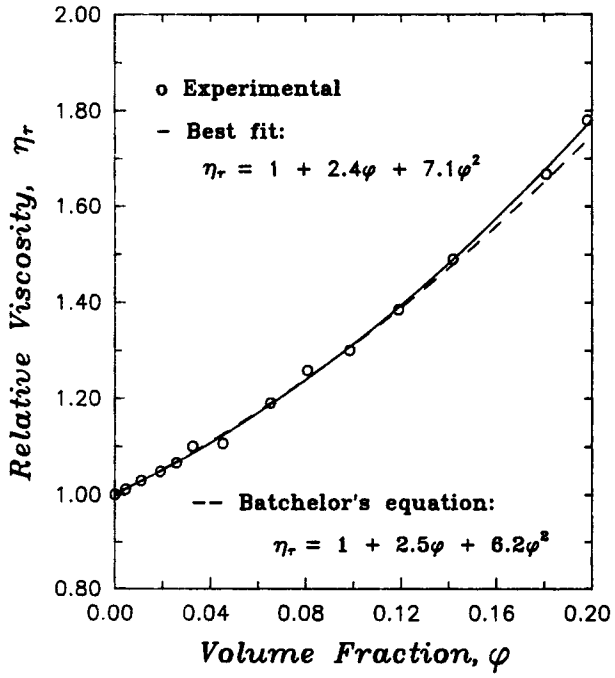

Figure 3. Relative viscosity of silica suspensions as a function of particle volume fraction.

in the concentration range $0 < C < 0.36$ gm/cm^3 at 25°C ± 0.1°C. The measurements were carried out in a Brookfield viscometer at three different shearing rates. For $C < 0.36$ gm/cm^3, the viscosity of the suspensions was found to be independent of the shearing rates and the suspensions behaved as Newtonian fluids. For higher concentrations ($\phi > 0.25$), however, shear thinning was observed. These results are in agreement with the work of Krieger (1972) who found shear thinning to be detectable only for $\phi > 0.25 - 0.30$. Very accurate viscosity data were next obtained using Cannon-Fenske tubes immersed in a water bath at 25 ± 0.1°C. The experimental data in the dilute concentration range ($0 < C < 0.049$) were fitted to the Einstein relation:

$$\frac{\eta}{\eta_0} = 1 + 2.5\phi \tag{11}$$

and the value of $\bar{v}_h$ for the particles was accordingly determined. The viscosity data over the concentration range $0 < \phi < 0.2$ are shown in Figure 3. The viscosity data are needed in the experimental determination of the diffusion coefficient of the particles at finite concentrations. A fit to these data by a second degree polynomial gives

$$\frac{\eta}{\eta_0} = 1 + 2.4\phi + 7.1\phi^2 \tag{12}$$

The coefficients in this equation are in fairly good agreement with the theoretical values of 2.5 and 6.2 obtained by Einstein (1906) and Batchelor (1977), respectively. This curve fitting procedure may be objected to on the grounds that the Einstein value of 2.5 was used to obtain $\bar{v}_h$ from the low concentration data. A second curve fit of the data was therefore made forcing the coefficient of the linear term to be 2.5. The resulting expression is

$$\frac{\eta}{\eta_0} = 1 + 2.5\phi + 6.54\phi^2 \tag{13}$$

The value 6.54 for the $O(\phi^2)$ coefficient is now in better agreement with Batchelor's value.

Diffusion experiments were performed at 25 ± 0.1°C in the concentration range between $C = 0.00803$ and 0.3599 g/cm^3. Details regarding these measurements are described in the experimental section. The diffusion data extrapolated to zero concentration provided the Stokes-Einstein coefficient D_0. The measured value for D_0 was next used in the Stokes-Einstein equation to determine the hydrodynamic radius a_h of the particles. A summary of the properties of the particles in cyclohexane are given in Table 3. From this table we note that $\bar{v}_t$ is less than $\bar{v}_h$ and a_{EM} is also less than a_h. An explanation for the difference between $\bar{v}_t$ and $\bar{v}_h$ can be found in considering the silica particle itself. It consists of a nucleus of silicon dioxide, that may contain small pores, which can be filled with solvent when dispersing the particles. The nucleus is surrounded by a spherical shell of hydrocarbon chains, which also contains solvent. Furthermore, the outer surface of the particle is not truly spherical and solvent may be carried in the surface irregularities as the particle moves in the dispersion. We therefore expect that the thermodynamic volume of the particles

will be smaller than the hydrodynamic volume of the "quasihard" spherical particles, that is, $\bar{v}_l$ will always be less than $\bar{v}_h$. Noting that the hydrodynamic volume is that volume that is displaced as the particle moves in the dispersion, we also expect that a_{EM} will be less than a_h. The decrease in particle radius is also a result of radiation damage that occurs during the electron microscopy measurements. A slight difference is therefore expected, because the aliphatic chain molecules will be expanded in a good solvent, contrary to a more collapsed configuration in the dry phase.

Osmotic pressure measurements of the particles dispersed in cyclohexane were also carried out in the concentration range $0<\phi<0.37$ using a Knauer High Speed Membrane Osmometer. The osmometer has five pressure ranges (0–2.5, 0–5, 0–10, 0–20, and 0–40 cm of solvent) and requires a chart recorder with a 100 mV full-scale range. One obtains the osmotic pressure as centimeters of solvent from the graph on the chart recorder. For a 10-in. (25-cm) chart recorder, the 0–2.5 cm scale is the most sensitive scale available. Pressure readings varied from about 0.3 cm solvent for the lowest concentration used ($\phi \simeq 0.05$) to about 10 cm solvent for the highest concentration ($\phi \simeq 0.37$). The readings could be read accurately to within 0.5% of the full-scale range. Three to four measurements were made at each concentration. For $\phi > 0.1$, reproducibility of the measurements varied between 4 and 10%. For $\phi < 0.1$, however, reproducibility varied between 20 and 30% indicating that the instrument became less accurate when the osmotic pressure fell below 1 cm of solvent. Reconditioned deacetylated cellulose acetate membranes were used in all runs. The experimental results are shown in Figure 4. Theoretical predictions for the osmotic pressure from the Carnahan-Starling equation are also shown in this figure. As can be seen, the agreement between the experimental data and theoretical predictions is fairly good; thereby providing a direct evidence to the hard-sphere nature of our silica system.

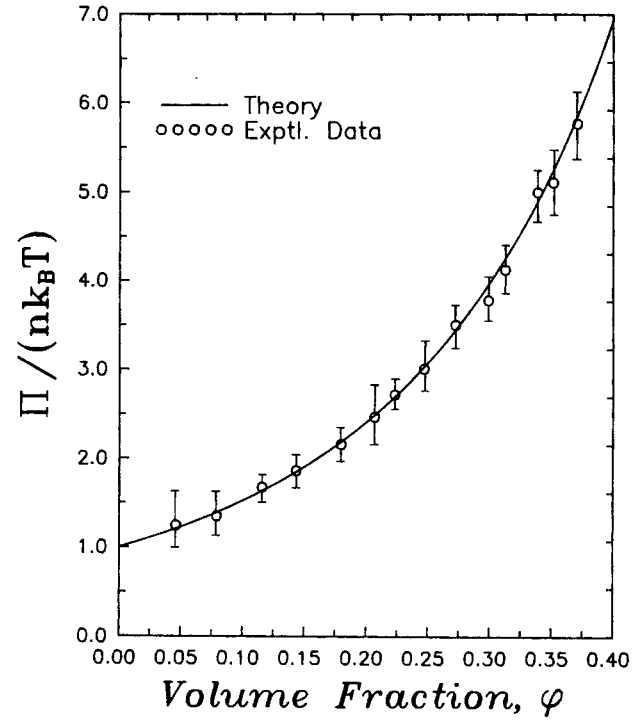

Figure 4. Reduced osmotic pressure of silica suspensions as a function of particle volume fraction.

Experimental

Apparatus and procedure

The experimental setup used in measuring the diffusion coefficients is shown in Figure 5. The main parts are a solution cell and a capillary tube. The solution cell consists of a reservoir (plexiglass cylinder) 5.7 cm in height and 3.3 cm in diameter and equipped with a plexiglass lid which has an off-center bore through which a 2-mm slanted-tip glass tube is permanently connected. This tube is used to fill the reservoir with the more dense solution via a variable speed pump. The capillary tube is precision bore glass of known radius and length greater than the maximum penetration depth of any experiment. The capillary is fitted at the bottom with a Luer-Lok microvalve to facilitate filling and emptying. The capillary is open at the top and connected to the plexiglass reservoir using a special threaded plug. An O-ring is used to ensure the capillary-reservoir seal. The reservoir-capillary system was mounted on a rigid support and the whole assembly was mounted on a vibration-free optical table. The assembly was installed in a constant temperature air bath maintained at 25 ± 0.1°C.

Prior to each experiment, the solution cell and the capillary tube were rinsed several times with the appropriate solvent (distilled water or cyclohexane) depending on the type of experiment. The setup was assembled as in Figure 5 and verticality

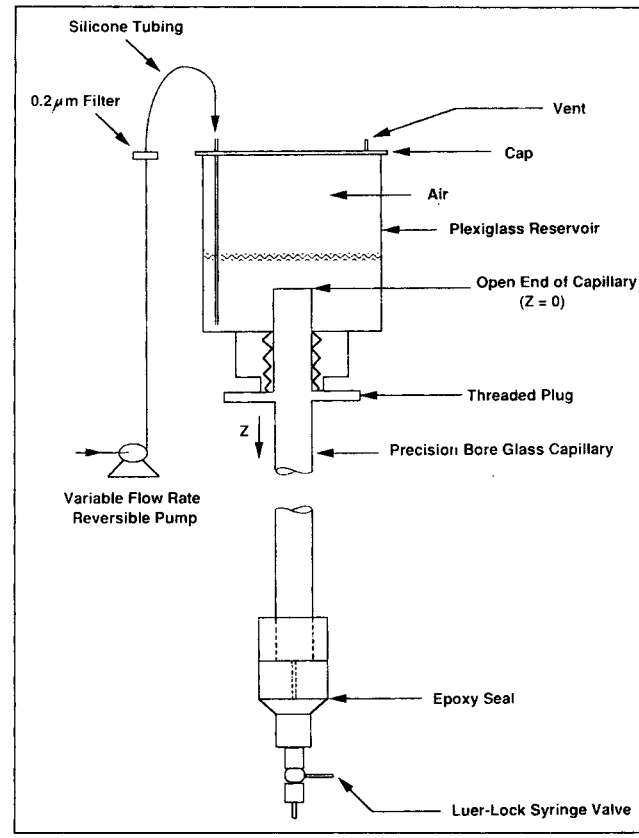

Figure 5. Apparatus for measuring the diffusion coefficient through stabilization of an inverse density gradient.

of the capillary tube was checked and adjusted using a cathetometer. The microvalve at the lower end of the capillary tube was connected to a silicone tubing, and the less dense solution was injected very slowly into the capillary tube using a variable speed pump. Extreme caution was taken so that no air bubbles could be trapped inside the capillary tube after the filling process. The filling of the capillary stopped as soon as the liquid covered the reservoir-end of the capillary. Care was taken to ensure that the capillary was completely filled with no liquid spillover on the floor of the solution cell. Immediately afterwards, the reservoir was slowly filled with the more dense solution using a variable speed pump. The careful (slow) filling of the reservoir with the dense solution was very important to prevent overshoot problems. To achieve this, the initial contacting of reservoir and capillary fluids was done very slowly with minimum convection currents in the reservoir. As soon as the solution in the reservoir covered the top of the capillary, free convection started. The reservoir-capillary arrangement was allowed to sit for a minimum period of time to ensure that hydrodynamic stability has been reached. The durations of the experiments, at 25°C, were approximately 3–6 and 120 hours for the aqueous solutions and colloidal suspensions respectively. These periods were long enough for the convection to be complete but not so long as to let longitudinal diffusion significantly affect the results. During the experiments the penetration depth was monitored using a laser-excited fluorescent dye tracer. This technique is described below in detail.

In all cases the solution level in the reservoir was at least 1 cm higher than the position of the open end of the capillary so that disturbances at the air/solution interface could not propagate into the capillary. Moreover, the volume of fluid in the reservoir was much greater than that in the capillary to maintain a constant reservoir concentration during the displacement of fluid from the capillary into the reservoir.

Measurement of penetration depth and concentration profile

To monitor the penetration depth and/or the concentration profile during the convection process, a laser-excited fluorescent dye tracer was added to the reservoir fluid. If the tracer is sufficiently dilute, it will mix in the capillary by convection in the same proportion as in the reservoir. Thus measurement of the tracer concentration is equivalent to measurement of the solute concentration. Molecular diffusion would lead to disproportionate mixing, but the timescale for this to occur is of orders of magnitude longer than the convective process. A mathematical criterion which provides an upper limit on the concentration of the tracer added to the reservoir fluid without introducing a third component to the system was derived and experimentally verified by Lowell and Anderson (1982). This criterion is also discussed in the review by Quinn et al. (1986). In all our experiments, this criterion was always satisfied.

The tracer chosen for our experiments was rhodamine 6G which is a fluorescent dye having an absorption band in the range of 480–580 nm wavelength. Fluorescence is emitted in a broadband centered at about 590 nm wavelength and is excited by an argon-ion laser at 488 nm or a He-Ne laser (green) at 554 nm. The following two methods for excitation and detection were developed in the present work.

In the first method, a light beam from a 1 mW He-Ne (green) laser (wavelength = 554 nm) passes through a set of cylindrical lenses. These lenses convert the 0.62 mm diameter beam to a horizontal slit of parallel rays approximately 0.5 cm wide and 0.06 cm high. The flat beam is focused on the capillary tube. The laser and the lenses were mounted on one side of the capillary tube on a horizontal support. This support is connected to a vertical screw shaft which is driven by a reversible stepper motor controlled through a microcomputer. The laser optics assembly can be moved up and down the diffusion column by means of the stepper motor. To visually detect the penetration depth of the dye in the diffusion column, a laser goggle is used which makes the fluorescent light (orange) from the dye visible but not the excitation light (green). During the experiment, the convective (penetration) front can be traced visually by means of the fluorescent light using the traveling laser system and the goggle. With the penetration front located, the penetration distance is measured using a cathetometer.

In the second method, laser excitation is transmitted to the dye in the diffusion column by optical fibers and fluorescence radiation from the dye is carried out by optical fibers to a filter/detector module. The basis of this technique is to measure the concentration profile of the tracer dye vs. time along the diffusion column nonintrusively. Laser excitation is transmitted to five fixed sampling positions along the capillary by optical fibers. Excitation of 1 mW is directed onto the clamped cleaved ends of this bundle of 5 fibers each of 200 micron core diameter and 230 micron cladding diameter. At the capillary, each fiber terminates in a transparent acrylic sampling clamp illustrated in Figure 6. Since the excitation emerging from each fiber termination diverges at a numerical aperture of 0.37 for the fibers used here, a collimating lens is used to illuminate the capillary with parallel light at each sampling point. For this, a graded-refractive-index (GRIN) lens of 2 mm dia. is used. To collect the fluorescence from the same capillary volume, two similar GRIN lenses and fibers are inserted in each clamp arrangement and positioned so as not to receive excitation directly from the excitation fiber. In this arrangement, the collection fibers receive fluorescence at an angle of 75° from the excitation direction.

Fluorescence radiation collected at each sampling clamp is carried by fibers to a filter/detector module shown in Figure 7. These modules were built to the design specifications reported by Perkins and Jones (1989). In each module, fluorescence emerging from each of the collection fibers is first collimated by a GRIN lens and directed at normal incidence onto a long-wave-pass dichroic filter. It was designed to block the excitation wavelength. A second band-pass filter is used to reject broad band fluorescence from other components in the optical path. It is centered at 590 nm and has a 30 nm band width. Finally, the transmitted fluorescence impinges on a silicon photodiode detector (Hamamatsu S1226-18BQ). This is an extremely low-noise optical detector having a Noise Equivalent Power (NEP) of 10^{-15} W/Hz$^{1/2}$ and a sensitivity of 0.38 W/A. Operational amplifiers (Burr-Brown OPA 128) with ultralow-bias current monitor the photodiodes. The amplifiers operate in the current-to-voltage mode with 10 GΩ feedback resistors and have FET inputs with an input bias current of 150 fA as required for the large feedback resistor. The five operational amplifier circuits and silicon diode detectors are mounted on a single 130 by 150 mm circuit card designed to hold 16 such circuits. The maximum crosstalk

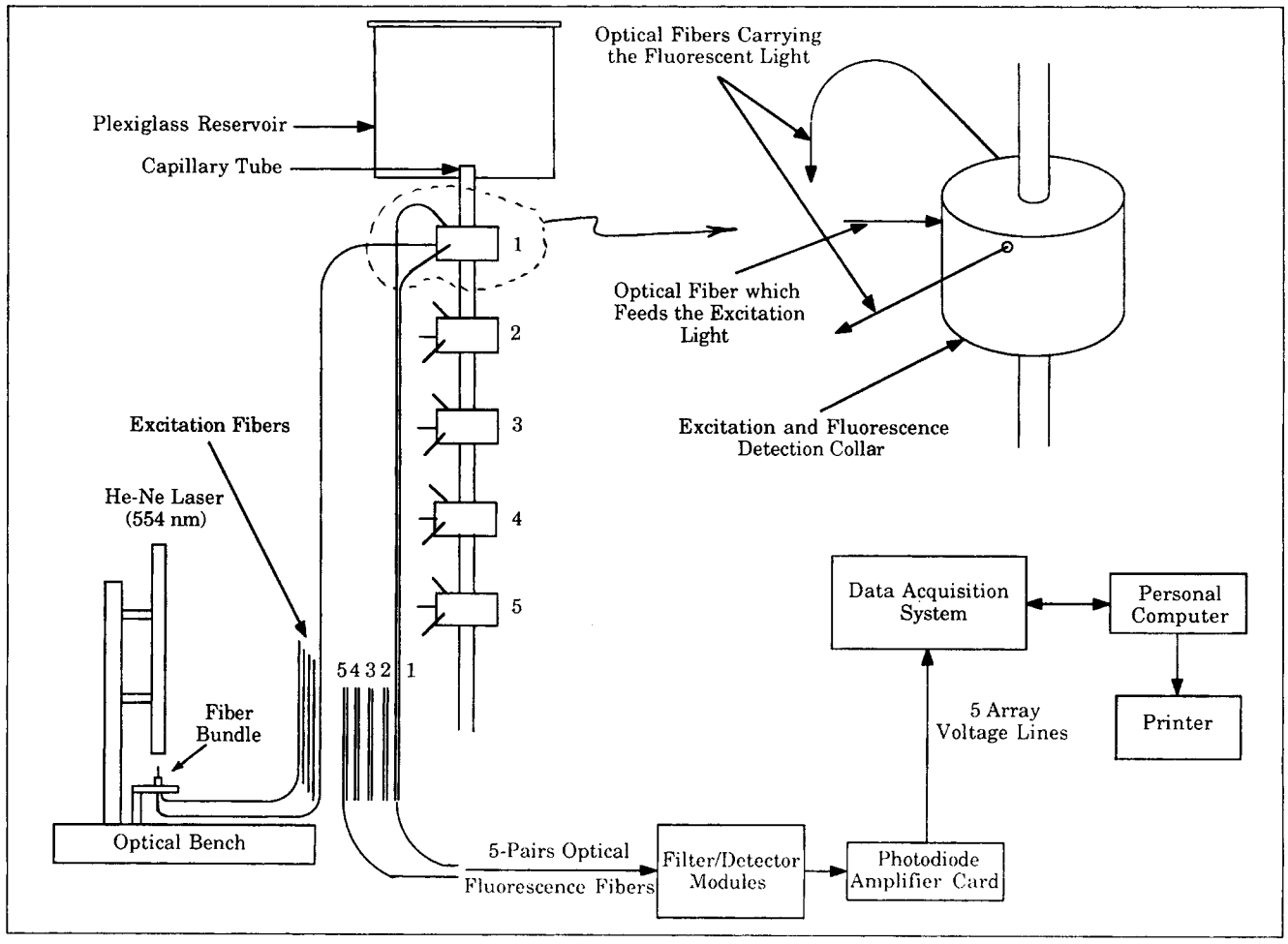

Figure 6. Overview of the fluorescent technique assembly.

between circuits was determined by Perkins and Jones (1989) for similar cards to be less than 40 dB.

A programmable data acquisition system is used to log the fluorescence detector outputs in conjunction with a personal computer. A computer program selects each operational amplifier output in turn to be processed by a 12 bit analog-to-digital converter. Typically, the five outputs are stored in the computer memory at intervals of 60 s. During preliminary calibration runs, the outputs are sampled for a period of 300 s at 1 s intervals. The mean and standard deviation of the signals are computed over this period. The full-scale output for a signal of 10 ppm tracer dye for each channel is about 20 mV with standard deviation of 0.24 mV. On the bases of these calibration runs, the experimental precision for concentration is estimated to be 0.12 ppm ($=\sigma$).

At the dilution levels of the tracer dye used in these experiments, about 10 ppm, the fluorescence intensity was found to be linear with concentration. In view of this linearity it was considered sufficient to calibrate each sampling assembly at two concentrations. Calibration of the fluorescence detector array was carried out in situ in order to allow for differences in the individual fluorescence probes.

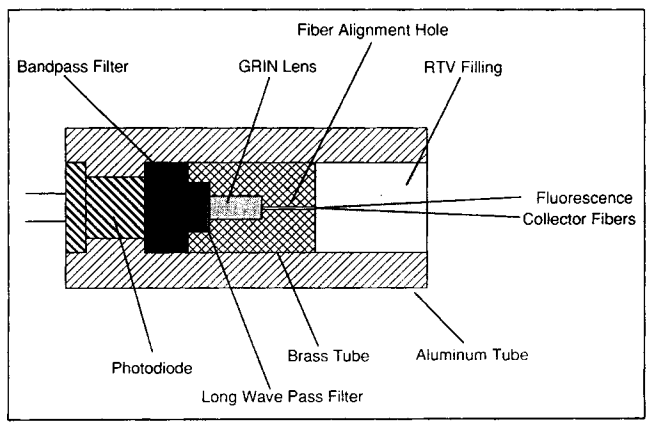

Figure 7. Cross-section of a coupler-detector module.

Preparation of aqueous solutions and silica dispersions

Aqueous solutions of sucrose, sodium sulfate, and potassium chloride with known diffusion coefficients were used to test the tracer-dye methods developed in the present work. In preparing these solutions, a known weight of the solute was dissolved in a stock solvent to achieve the desired concentration. The stock solvent consisted of rhodamine 6G dissolved in deionized and doubly-distilled water. The concentration of

the rhodamine dye in the stock solvent was maintained at 10 ppm when using the fiber-optic technique and 1 ppm when using the visual technique.

In the diffusion experiments with hard spheres, a small amount of silica particles was dispersed in a chloroform-rhodamine solution where the concentration of rhodamine was no more than 1 ppm. (Rhodamine 6G dissolves readily in chloroform but is insoluble in cyclohexane.) The suspension was shaken periodically and let stand overnight in order to load or absorb some of the rhodamine molecules on the surface of the particles. The particles were then separated from the chloroform-dye solution, washed once with pure chloroform and twice with pure cyclohexane, and dried under nitrogen atmosphere for 24 hours at 80°C. These rhodamine-tagged particles were used as tracers to track the penetration depth in the diffusion experiments. In preparing a silica dispersion for these experiments, known weights of rhodamine-free particles and rhodamine-tagged particles were dispersed in cyclohexane to achieve the desired particle concentration. The weight ratio of tagged to untagged particles was maintained at about 0.005. All solutions and dispersions were used promptly after their preparation.

Computation of the diffusion coefficient

Consider a reservoir of dense solution with solute and tracer dye at constant concentrations of C_0 and C_0^*, respectively. Similarly, let C_1 and C_1^* represent the initial concentrations of the solute and the tracer dye in the less dense solution in the capillary. When the reservoir solution contacts the less dense solution at the top of the tube, the reservoir and tube fluids mix until marginal stability is attained. Assuming that the solute and the tracer dye diffuse independently, the marginal stability criterion is given by (Wooding, 1959):

$$-\frac{ga_c^4}{\eta(\bar{C})}\left[\frac{\alpha}{D(\bar{C})}\frac{dC}{dz}+\frac{\alpha^*}{D^*(\bar{C}^*)}\frac{dC^*}{dz}\right]=67.94 \qquad (14)$$

where z is directed downwards along the tube, a_c is the inner radius of the tube, g is the gravitational acceleration, α and α^* are respectively the density coefficients of the solute and tracer dye, $\eta(\bar{C})$ is the viscosity of the solution in the capillary, and D and D^* are the diffusion coefficients of the solute and tracer dye, respectively. The quantities η, D, and D^* are determined at the local concentrations in the capillary, $\bar{C}$ and $\bar{C}^*$. Generally, small concentration differences are maintained between the reservoir and the capillary so that $\bar{C}$ and $\bar{C}^*$ may be approximated by their mean values: that is, $\bar{C}=(C_0+C_1)/2$ and $\bar{C}^*=(C_0^*+C_1^*)/2$.

Assuming that both solute and tracer dye are convected to the same depth L_c in the tube, Eq. 14 can be integrated to the penetration depth at marginal stability as:

$$L_c=\frac{ga_c^4}{67.94\eta(\bar{C})}\left[\frac{\alpha(C_0-C_1)}{D(\bar{C})}+\frac{\alpha^*(C_0^*-C_1^*)}{D^*(\bar{C}^*)}\right] \qquad (15)$$

where L_c is the distance down the tube where the concentrations of the solute and the tracer dye become equal to C_1 and C_1^*, respectively. Equation 15 assumes linear concentration profiles for both solute and tracer dye within the capillary at marginal stability. The correctness of this equation was demonstrated experimentally by Lowell and Anderson (1982). When the tracer dye concentration is sufficiently small so that

$$\frac{\alpha(C_0-C_1)}{D(\bar{C})}>>\frac{\alpha^*(C_0^*-C_1^*)}{D^*(\bar{C}^*)},$$

Equation 15 simplifies to

$$D(\bar{C})=\frac{\alpha g a_c^4}{67.94\eta(\bar{C})}\frac{(C_0-C_1)}{L_c} \qquad (16)$$

This equation was used throughout the present work to calculate the diffusion coefficient as a function of concentration from the measured penetration depth L_c. The density coefficient α ($=\partial\rho/\partial C$ where ρ is the density of the solution) and the viscosity $\eta(\bar{C})$ for the aqueous solutions used in the present work were obtained from the literature. For silica dispersions, the partial specific volume of the particles $\bar{v}_h$ is independent of the concentration of the particles in the suspension. Accordingly, the density of the dispersion could be related to the particle concentration C via the relationship:

$$\rho=\rho_0+(1-\bar{v}_h\rho_0)C \qquad (17)$$

where ρ_0 is the density of the solvent (cyclohexane). The density coefficient α for silica dispersions was therefore readily obtained from:

$$\alpha=1-\bar{v}_h\rho_0 \qquad (18)$$

Results and Discussion

Diffusion coefficients of aqueous solutions using the visual method

Using different sizes of capillaries, the diffusivities of sucrose, sodium sulfate, and potassium chloride solutions were measured at different concentrations ranging from 0.004 to 0.7 molar. All of the experimental diffusivity data were obtained at 25°C. For each run, the penetration front, which was observed to be fairly sharp, was monitored visually using the goggle and traveling laser assembly as described earlier. The reproducibility of the transient data of penetrating fronts is illustrated in Figure 8 for a sucrose solution with $C_0=0.04504$ g/cm^3 and $C_1=0$. Similar plots were also obtained for sodium sulfate and potassium chloride solutions. In Figure 8, the rising portion of the curve represents the early stages of the movement of the penetration front while the horizontal portion represents the attainment of marginal stability.

Table 4 summarizes the experimental results for the diffusion coefficients using the visual technique. A glance at this table reveals a remarkable agreement of our data with data reported in the literature. The average deviation is less than 4%.

Diffusion coefficients of aqueous solutions using the fiber-optic system

Diffusion coefficient measurements were also performed for the aqueous solutions using the fiber-optic system described

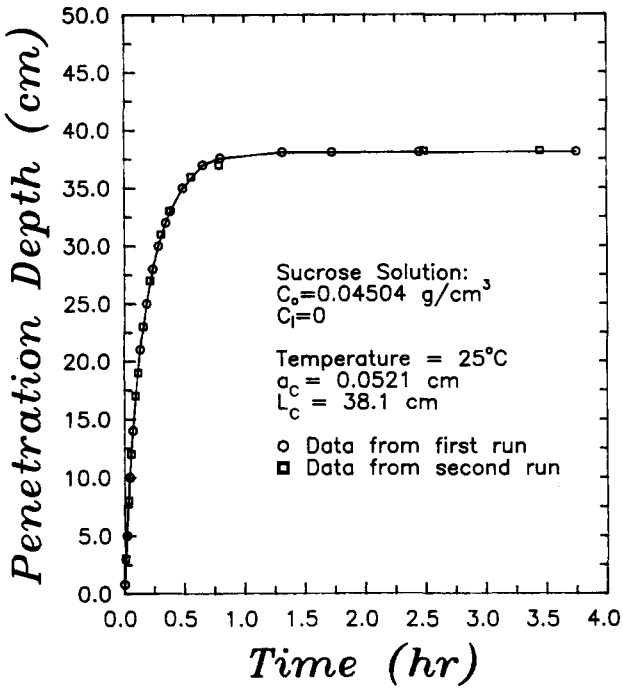

Figure 8. Penetration depth vs. time for a sucrose solution with $C_0 = 0.04504$ gm/cm^3 and $C_i = 0$.

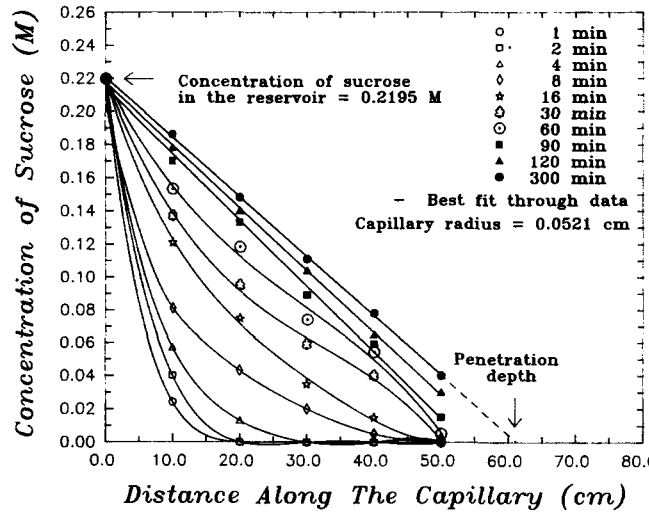

Figure 9. Transient concentration profiles along the capillary tube for a sucrose solution with $C_0 = 0.07507$ gm/cm^3 and $C_i = 0$.

earlier. Due to space limitation, only sample results are presented. Figure 9 shows the transient concentration profiles along the capillary for a sucrose solution with $C_0 = 0.07507$ g/cm^3 and $C_i = 0$. The solid lines in this figure represent the best-fit curves through the data. As can be seen, a linear concentration profile is attained at stable conditions after about 300 minutes. Extrapolation of this profile to zero concentration (the initial concentration in the capillary) determines the stable penetration depth. Diffusion coefficient measurements based on this technique are listed for two sucrose concentrations in Table 5. Overall, these measurements are about 1.6% higher than those found by the visual method reported above. It is clear however from the table that both methods yield values for D which are sufficiently accurate to test the theory of diffusion of colloidal particles.

Table 4. Experimental Results for Diffusion Coefficients of Aqueous Solutions

Molar Conc.	$D \times 10^5$ (cm^2/s) Exp.	Lit.*	% Dev.
	Sucrose		
0.0219M	0.5095	0.5168	−1.41
0.0293M	0.5085	0.5149	−1.24
0.0659M	0.4999	0.5052	−1.05
0.1098M	0.4898	0.4936	−0.77
0.1536M	0.4808	0.4820	−0.25
	Sodium Sulfate		
0.00268M	1.138	1.151	−1.13
0.00356M	1.120	1.137	−1.50
0.00448M	1.107	1.129	−1.95
0.00479M	1.092	1.124	−2.85
	Potassium Chloride		
0.00194M	1.921	1.954	−1.69
0.00585M	1.883	1.931	−2.49
0.00980M	1.866	1.918	−2.71
0.04620M	1.818	1.872	−2.88
0.06074M	1.798	1.856	−3.13
0.12980M	1.774	1.838	−3.48
0.33230M	1.792	1.842	−2.71
0.52760M	1.828	1.852	−1.30

*Literature data are due to Gosting and Morris (1949), Harned and Nuttal (1949), and Harned and Blake (1951).

Diffusion coefficients of silica dispersions

Diffusion coefficients of our coated silica particles dispersed in cyclohexane were measured over the concentration range $0.0055 < \phi < 0.248$ using both the visual and the fiber-optic techniques. The data were collected at 24 different concentrations spanning this concentration range. For each concentration, the experiment was repeated at least four times and the mean value was used for the diffusion coefficient. Reproducibility was better than 4% of the mean value. During the experiments, the concentration C_0 of the particles in the reservoir was always less than 5 vol.% above the initial concentration C_i in the capillary. Figure 10 is a representative plot of the penetration depth down the capillary vs. time. At least 120 hours were needed to ensure that hydrodynamic stability had been reached. Figure 11 is a representative plot of the measured concentration profile of the silica particles within the capillary at stable conditions.

Experimental results for the diffusion coefficient of silica

Table 5. Fiber-Optic Technique vs. Visual Method for Measuring Diffusion Coefficient of Aqueous Sucrose Solutions

Concentration	$D \times 10^6$ (cm^2/s) Fiber-Optic	Visual	Lit.*	%Dev. Fiber-Optic	Visual
0.06585 M	5.079	4.999	5.052	0.53	−1.05
0.10975 M	4.979	4.898	4.936	0.87	−0.77

*Literature data are due to Gosting and Morris (1949).

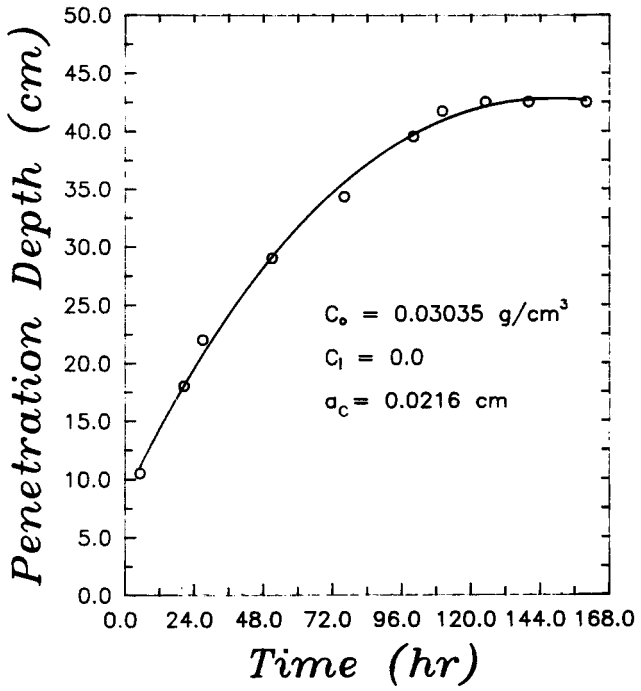

Figure 10. Penetration depth vs. time for a silica dispersion with $C_0 = 0.03035$ gm/cm^3 and $C_1 = 0$.

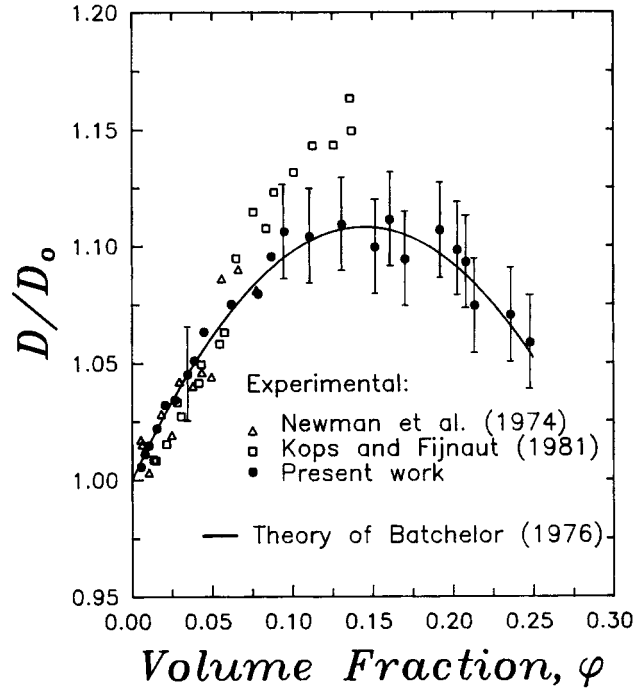

Figure 12. Experimental data for the diffusion coefficient of hard spheres vs. theoretical predictions due to Batchelor (1976).

dispersions as a function of particle concentration are presented in Figure 12. As can be seen the diffusion coefficient rises, more or less linearly with concentration, passes through a maximum between 0.13 and 0.16 volume fraction, and then decreases with concentration. The low concentration data with $\phi < 0.05$ (about 9 data points) were linearly extrapolated to zero concentration and D_0 was accordingly determined (see Table 3). The best-fit straight line through these data points gave an $O(\phi)$ coefficient of 1.39 ± 0.19 which is in fairly good agreement with Batchelor's theoretical value of 1.45.

The solid curve in Figure 12 represents theoretical predictions for the diffusion coefficient from the generalized Stokes-Einstein equation as derived by Batchelor (Eq. 8). In this equation, the sedimentation coefficient $K(\phi)$ is evaluated from

$$K(\phi) = (1-\phi)^{6.55} \tag{19}$$

and the osmotic compressibility is taken from the Carnahan-Starling equation as

$$\left(\frac{\partial \Pi}{\partial n}\right)_{T,P} = k_B T \frac{[(1+2\phi)^2 + (\phi-4)\phi^3]}{(1-\phi)^4} \tag{20}$$

Accordingly, Eq. 8 becomes

$$\frac{D}{D_0} = (1-\phi)^{6.55} \frac{[(1+2\phi)^2 + (\phi-4)\phi^3]}{(1-\phi)^4} \tag{21}$$

Expression 19 for $K(\phi)$ was verified experimentally by Al-Naafa and Selim (1992).

A glance at Figure 12 shows that the experimental data agree well with theoretical predictions at low concentrations. Slight deviations, however, are apparent at high concentrations. Nonetheless, the agreement between experimental results and theoretical predictions is within the repeatability of the ex-

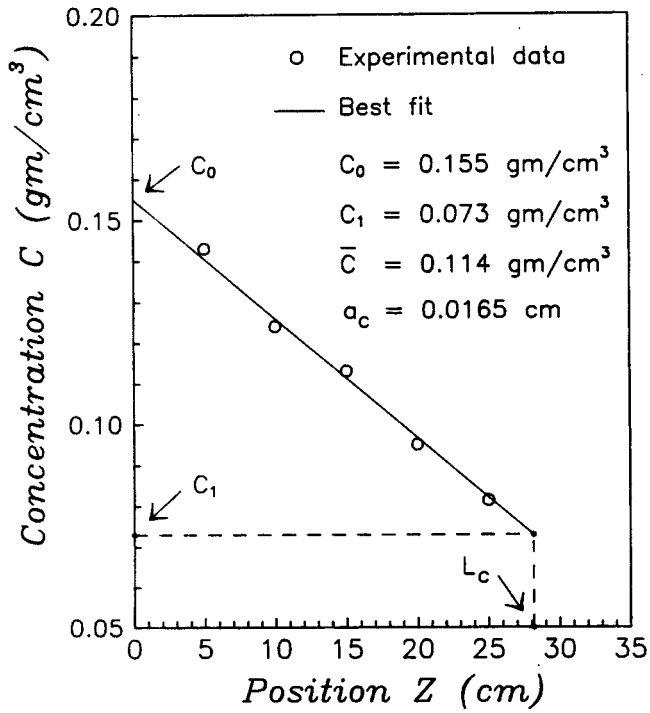

Figure 11. Measured concentration profile of silica particles within capillary at stable conditions.

perimental determinations over the entire concentration range studied.

Also included in Figure 12 are two sets of data due to Newman et al. (1974) and Kops-Werkhoven and Fijnaut (1981). Newman et al. (1974) measured the diffusion coefficient of single stranded circular DNA from the fd bacteriophage in aqueous solutions of high ionic strength [0.15 M NaCl-0.015 M sodium citrate (pH 8)]. Their aqueous DNA solutions were quite monodisperse with a hydrodynamic radius of 31 nm. Diffusion coefficients were measured by intensity fluctuation spectroscopy over the concentration range $0.0054 < \phi < 0.0775$. Kops-Werkhoven and Fijnaut (1981) measured the diffusion coefficient of sterically stabilized silica particles dispersed in cyclohexane. The suspensions were fairly monodisperse with a hydrodynamic radius of 23 nm. The measurement of D was performed using dynamic light scattering in the concentration range $0.0136 < \phi < 0.1371$. Both data sets produce an $O(\phi)$ coefficient which is in good agreement with Eq. 8 (see Table 1). However, for $\phi > 0.07$, the data by Kops-Werkhoven and Fijnaut diverge from Eq. 8 with the difference increasing markedly with concentration. These data were collected using dynamic light scattering which is an accurate technique at low concentrations. At finite concentrations, however, the technique suffers from the potential hazard of multiple scattering effects. Multiply scattered light experiences multiple frequency dispersion contributions, and if present to a significant degree, may lead to spurious increases in the Rayleigh line-width and hence artificial increases in derived diffusion coefficients. Such a phenomenon might, therefore, explain the large positive deviations associated with the data of Kops-Werkhoven and Fijnaut at finite concentrations. Mos et al. (1985) have developed an experimental scheme which suppresses multiple scattering in dynamic light scattering experiments. The technique uses the so-called cross-correlation function instead of the familiar auto-correlation function. The cross-correlation setup was used by Mos et al. (1986) to measure the diffusion coefficient of stearylated silica spheres in toluene and xylene. Their measurements gave an $O(\phi)$ coefficient which varied from -0.9 to -1.2 (see their Figures 5 and 6). These results are in substantial disagreement with the present results as well as with previous studies of Kops-Werkhoven and Fijnaut (1981) and Newman et al. (1974). Further experience with the cross-correlation technique is required before this discrepancy can be resolved.

Effect of Polydispersity

Polydispersity in size may have a pronounced effect on the static and hydrodynamic properties of colloidal suspensions. For our particle system, a size polydispersity of 13.1% was found from electron microscopy measurements (see Table 3). Because of the necessary pretreatment of the particles for such measurements and the possible radiation damage during the exposure, we believe that the real size distribution of the suspended particles in the dispersion will probably be narrower. Assuming however the same polydispersity for the suspended particles, we find the hydrodynamic radius a_h as 20.01 ± 2.6 nm. In order to ascertain the effect of such polydispersity in size on the experimental results for the diffusion coefficient, the total size range (17–23 nm) was divided into five equal size fractions. Each fraction i was represented by its midpoint radius a_i and had a concentration C_i equal to the total particle concentration C multiplied by the fractional probability p_i for the size fraction in question, which is equal to the area under the probability histogram between the lower and upper radii defining the size fraction. For this multisize system, Eq. 15 takes the form (Lowell and Anderson, 1982):

$$L_c = \frac{g a_c^4}{67.94\ \eta(\bar{C})} \sum_{i=1}^{5} \frac{\alpha_i (C_0 - C_1)_i}{D_i(\bar{C}_i)} \tag{22}$$

which assumes no coupling between diffusion of the particle species in the mixture and that all species are convected to the same depth L_c in the capillary. Equation 22 then is only applicable to dilute solutions where diffusive coupling is usually small. In this case the diffusion coefficient of the i-th particle species, $D_i(\bar{C}_i)$ may be approximated by $D_{0,i}(1 + k\bar{C}_i)$. The density coefficients, α_i's, in Eq. 22 were also taken equal to α, the density coefficient of the mixture. The low concentration data with $\phi < 0.05$ were reanalyzed using Eq. 22. The analysis yielded results for the first-order correction in D which were about 4 to 7% higher in comparison with the values obtained assuming negligible polydispersity. For high concentrations ($\phi > 0.05$), diffusive coupling among the various species in the mixture becomes important and Eq. 22 takes the form (Glendinning and Russel, 1980):

$$L_c = \frac{g a_c^4}{67.94\ \eta(\bar{C})} \sum_{i=1}^{5} \sum_{j=1}^{5} \frac{\alpha_i (C_0 - C_1)_j}{D_{ij}(\bar{C}_i, \bar{C}_j)} \tag{23}$$

where D_{ij} are the multicomponent diffusion coefficients. When coupling is negligible, $D_{ij} = 0$ for $i \neq j$ and $D_{ii} = D_i$ so that Eq. 23 reduces to Eq. 22. Because of the large number of unknowns in Eq. 23 and the meagerness of the data in the high concentration range (only 15 data points), it was not possible to estimate the D_{ij}'s with sufficient certainty. To a first approximation, however, the cross-term diffusion coefficients were neglected and only the main-term coefficients were retained. Results for the diffusion coefficient based on this approximation were again consistently higher by about 4 to 9% than those obtained assuming negligible polydispersity. Based on this preliminary analysis, the overall effect of taking the polydispersity of our particles into account results in slightly better agreement with Batchelor's theory. It will be desirable, however, to carry out a systematic study of multicomponent diffusion of hard spheres which takes into account the cross coefficients of the diffusion tensor. The foregoing discussion shows that the present experimental technique appears to be well suited for this purpose.

Acknowledgment

The authors wish to thank Dr. William B. Russel for helpful discussions during the execution of this work. Assistance of some members of the staff of the Transport Process Group, Chemical Engineering Division of the National Institute of Standards and Technology is also gratefully acknowledged.

Notation

a = particle radius
a_c = capillary tube radius
a_{EM} = particle radius from electron microscopy

a_h = hydrodynamic particle radius
C = solute or particle mass concentration
C_0 = solute or particle mass concentration in the reservoir
C_1 = initial mass concentration in the capillary
$\overline{C}$ = mean mass concentration in the capillary
C^* = tracer dye mass concentration
D = diffusion coefficient at finite concentration
D_0 = diffusion coefficient at infinite dilution
f = frictional coefficient at finite concentration
f_0 = frictional coefficient at infinite dilution
g = gravitational acceleration constant
k_B = Boltzmann constant
$K(\phi)$ = sedimentation coefficient
L_c = critical penetration depth
n = mean number density of the particles in the suspension
P = pressure
r = particle position vector at time t
r_0 = particle position vector at $t=0$
t = time
T = temperature
$\overline{v}_h$ = hydrodynamic specific volume
$\overline{v}_i$ = partial specific volume
z = distance along capillary axis toward higher gravitational potential

Greek letters

α = density coefficient ($=\partial\rho/\partial C$)
η = viscosity of solution or suspension
η_0 = viscosity of solvent or suspending medium
η_r = relative viscosity of suspension ($=\eta/\eta_0$)
Π = osmotic pressure
ρ = mass density of solution or suspension
ρ_0 = mass density of solvent or suspending liquid
ϕ = particle volume fraction

Literature Cited

Aguirre, J. L., and T. J. Murphy, "Brownian Motion of N Interacting Particles. II. Hydrodynamical Evaluation of the Diffusion Tensor Matrix," *J. Chem. Phys.*, **59**(4), 1833 (1973).

Al-Naafa, M. A., and M. S. Selim, "Sedimentation of Monodisperse and Bidisperse Colloidal Suspensions of Uncharged Rigid Spheres," *AIChE J.*, **38**(10), 1618 (1992).

Alpert, S. S., "Hydration Effects in the Diffusion of Spherical Macromolecules," *J. Chem. Phys.*, **65**, 4333 (1976).

Alpert, S. S., and G. Banks, "The Concentration Dependence of the Hemoglobin Mutual Diffusion Coefficient," *Biophys. Chem.*, **4**, 287 (1976).

Allison, S. A., E. L. Chang, and J. M. Schurr, "The Effects of Direct and Hydrodynamic Forces on Macromolecular Diffusion," *Chem. Phys.*, **38**, 29 (1979).

Altenberger, A. R., and J. M. Deutch, "Light Scattering from Dilute Macromolecular Solutions," *J. Chem. Phys.*, **59**(2), 894 (1973).

Altenberger, A. R., "On the Wave Vector Dependent Mutual Diffusion of Interacting Brownian Particles," *J. Chem. Phys.*, **70**, 1994 (1979).

Altenberger, A. R., J. S. Dahler, and M. V. Tirrell, "A Mean-Field Theory of Suspension Viscosity," *Macromolecules*, **18**, 2752 (1985).

Altenberger, A. R., and M. Tirrell, "Comments on Remarks on the Mutual Diffusion of Brownian Particles," *J. Chem. Phys.*, **84**, 6527 (1986).

Altenberger, A. R., J. S. Dahler, and M. Tirrell, "On the Molecular Theory of Diffusion and Heat Conduction in Multicomponent Solutions," *J. Chem. Phys.*, **86**, 2909 (1987).

Anderson, J. L., and C. C. Reed, "Diffusion of Spherical Macromolecules at Finite Concentration," *J. Chem. Phys.*, **64**(8), 3240 (1976).

Anderson, J. L., F. Rauh, and A. Morales, "Particle Diffusion as a Function of Concentration and Ionic Strength," *J. Phys. Chem.*, **82**, 608 (1978).

Ballard, C. C., E. C. Broge, R. K. Iler, D. S. John, and J. R. McWhorter, "Esterification of the Surface of Amorphous Silica," *J. Phys. Chem.*, **65**, 20 (1961).

Batchelor, G. K., "Sedimentation in a Dilute Dispersion of Spheres," *J. Fluid Mech.*, **52**(2), 245 (1972).

Batchelor, G. K., "Brownian Diffusion of Particles with Hydrodynamic Interaction," *J. Fluid Mech.*, **74**, 1 (1976).

Batchelor, G. K., "The Effect of Brownian Motion on the Bulk Stress in a Suspension of Spherical Particles," *J. Fluid Mech.*, **83**, 97 (1977).

Batchelor, G. K., "Diffusion in a Dilute Polydisperse System of Interacting Spheres," *J. Fluid Mech.*, **131**, 155 (1983).

Beenakker, C. W. J., and P. Mazur, "Diffusion of Spheres in Suspensions: Three-Body Hydrodynamic Interactions," *Phys. Letters*, **91**, 290 (1982).

Beenakker, C. W. J., and P. Mazur, "Self-Diffusion of Spheres in a Concentrated Suspension," *Physica 120A*, 388 (1983).

Berne, B., and R. Pecora, *Dynamic Light Scattering*, Wiley, New York (1976).

Dickinson, E., "Dispersions of Interacting Colloidal Particles," in the Annual Reports of the Progress of Chemistry (Physical Chemistry), The Royal Society of London, **80**, 3 (1983).

Einstein, A., "Investigations on the Theory of the Brownian Movement," *Ann. Physik*, **17**, 549 (1905).

Einstein, A., "A New Determination of Molecular Dimensions," *Ann. Physik*, **19**, 289 (1906).

Fair, B. D., D. Y. Chao, and A. M. Jamieson, "Mutual Transtational Diffusion Coefficients in Bovine Serum Albumen Solutions Measured by Quasielastic Laser Light Scattering," *J. Colloid Interface Sci.*, **66**(2), 323 (1978).

Felderhof, B. U., "Diffusion of Interacting Brownian Particles," *J. Phys. A: Math. Gen.*, **11**(5), 929 (1978).

Glendinning, A. B., and W. B. Russel, "A Pairwise Additive Description of Sedimentation and Diffusion in Concentrated Suspensions of Hard Spheres," *J. Colloid Interface Sci.*, **89**(1), 124 (1982).

Glendinning, A. B., and W. B. Russel, personal communication (1980).

Gosting, L. J., and M. S. Morris, "Diffusion Studies on Dilute Aqueous Sucrose Solutions at 1 and 25°C with the Gouy Interference Method," *J. Am. Chem. Soc.*, **71**, 1998 (1949).

Harned, H. S., and C. A. Blake, "The Diffusion Coefficients of Lithium and Sodium Sulfates in Dilute Aqueous Solutions at 25°C," *J. Am. Chem. Soc.*, **73**, 2448 (1951).

Harned, H. S., and R. L. Nuttal, "The Differential Diffusion Coefficient of Potassium Chloride in Aqueous Solutions," *J. Am. Chem. Soc.*, **71**, 1460 (1949).

Harris, S., "Diffusion Effects in Solutions of Brownian Particles," *J. Phys. A: Math. Gen.*, **11**, 1895 (1976).

Hess, W., and R. Klein, "Theory of Light Scattering from a System of Interacting Brownian Particles," *Physica*, **A85**, 509 (1976).

Iler, R. K., "Silica Hydrosol Powder," U.S. Patent 2,801,185 (1957).

Jones, C. R., C. S. Johnson, and J. T. Penniston, "Photon Correlation Spectroscopy of Hemoglobin: Diffusion of Oxy-HbA and Oxy-HbS," *Biopolymers*, **17**, 1581 (1978).

Keller, K. H., E. R. Canales, and S. Yum, "Tracer and Mutual Diffusion Coefficients of Proteins," *J. Phys. Chem.*, **75**(3), 379 (1971).

Kops-Werkhoven, M. M., and H. M. Fijnaut, "Dynamic Light Scattering and Sedimentation Experiments on Silica Dispersions at Finite Concentrations," *J. Chem. Phys.*, **74**, 1618 (1981).

Krieger, I. M., "Rheology of Monodisperse Latices," *Adv. Colloid Interface Sci.*, **3**, 111 (1972).

Lin, C. H., "Hydrodynamic Properties of Macromolecules as Determined from Stability Studies," PhD Thesis, University of Illinois, Urbana (1971).

Lowell, M. E., and J. L. Anderson, "Stable Concentration Gradients in a Vertical Tube," *Chem. Eng. Commun.*, **18**, 93 (1982).

Mewis, J., W. J. Frith, T. A. Strivens, and W. B. Russel, "The Rheology of Suspensions Containing Polymerically Stabilized Particles," *AIChE J.*, **35**, 415 (1989).

Mos, H. J., C. Pathmamanoharan, J. K. G. Dhont, and C. G. de Kruif, "Scattered Light Intensity Cross Correlation. II. Experimental," *J. Chem. Phys.*, **84**, 45 (1986).

Newman, J., H. L. Swinney, S. A. Berkowitz, and L. A. Day, "Hydrodynamic Properties and Molecular Weight of fd Bacteriophage DNA," *Biochemistry*, **13**(23), 4832 (1974).

Pecora, R., (ed.), *Dynamic Light Scattering: Applications of Photon Correlation Spectroscopy*, Plenum Press, New York (1985).

Perkins, R. A., and M. C. Jones, "Fiber-Optic Fluorescence Array

to Study Free Convection in Porous Media," *Rev. Sci. Instrum.*, **60**, 3492 (1989).
Phillies, G. D. J., G. B. Benedek, and N. A. Mazer, "Diffusion in Protein Solutions at High Concentrations: A Study by Quasielastic Light Scattering," *J. Chem. Phys.*, **65**, 1883 (1976).
Phillies, G. D. J., "Numerical Interpretation of the Concentration Dependence of Micelle Diffusion Coefficients," *J. Colloid Interface Sci.*, **119**, 518 (1987).
Prigogine, I., and R. Defay, *Chemical Thermodynamics*, John Wiley & Sons, New York (1954).
Pusey, P. N. and R. J. A. Tough, "Langevin Approach to the Dynamics of Interacting Brownian Particles," *J. Phys. A: Math. Gen.*, **15**, 1291 (1982).
Pusey, P. N., H. M. Fijnaut, and A. Vrij, "Mode Amplitudes in Dynamic Light Scattering by Concentrated Liquid Suspensions of Polydisperse Hard Spheres," *J. Chem. Phys.*, **77**, 4270 (1982).
Pusey, P. N., and R. J. A. Tough, "Particle Interactions," in *Dynamic Light Scattering*, by R. Pecora (ed.), pp. 85–179, Plenum Press, New York (1985).
Quinn, J. A., C. H. Lin, and J. L. Anderson, "Measuring Diffusion Coefficients by Taylor's Method of Hydrodynamic Stability," *AIChE J.*, **32**(12), 2028 (1986).
Russel, W. B., "Brownian Motion of Small Particles Suspended in Liquids," *Ann. Rev. Fluid Mech.*, **13**, 425 (1981).
Russel, W. B., D. A. Saville, and W. R. Schowalter, *Colloidal Dispersions*, Cambridge University Press, New York (1989).
Safran, S. A., and N. A. Clark (eds.), *Physics of Complex and Supermolecular Fluids*, Wiley-Interscience, New York (1987).
Schmitz, K. S., *An Introduction to Dynamic Light Scattering by Macromolecules*, Academic Press, Boston (1990).
Stöber, W., A. Fink, and E. Bohn, "Controlled Growth of Monodisperse Silica Spheres in the Micron Size Range," *J. Colloid Interface Sci.*, **26**, 62 (1968).
Taylor, G. I., "Conditions Under Which Dispersion of a Solute in a Stream of Solvent Can be Used to Measure Molecular Diffusion," *Proc. Royal Soc. (London)*, **A225**, 473 (1954).
van Helden, A. K., J. W. Jansen, and A. Vrij, "Preparation and Characterization of Spherical Monodisperse Silica Dispersions in Nonaqueous Solvents," *J. Colloid Interface Sci.*, **18**(2), 354 (1981).
Vrij, A., "Mixtures of Hard Spheres in the Percus-Yevick Approximation—Light Scattering at Finite Angles," *J. Chem. Phys.*, **71**, 3267 (1979).
Vrij, A., J. W. Jansen, J. K. G. Dhont, C. Pathmamanoharan, M. M. Kops-Werkhoven, and H. M. Fijnaut, "Light Scattering of Colloidal Dispersions in Non-Polar Solvents at Finite Concentrations," *Faraday Discuss. Chem. Soc.*, **76**, 19 (1983).
Wills, P. R., "Isothermal Diffusion and Quasielastic Light-Scattering of Macromolecular Solutes at Finite Concentrations," *J. Chem. Phys.*, **70**(2), 5865 (1979).
Wooding, R. A., "The Stability of a Viscous Liquid in a Vertical Tube Containing Porous Material," *Proc. Royal Soc. (London)*, **A252**, 120 (1959).

Manuscript received Aug. 16, 1991, and revision received July 20, 1992.